

## Investigating the microenvironments of inhomogeneous soft materials with multiple particle tracking

M. T. Valentine,<sup>1</sup> P. D. Kaplan,<sup>2</sup> D. Thota,<sup>3</sup> J. C. Crocker,<sup>3,\*</sup> T. Gisler,<sup>4</sup> R. K. Prud'homme,<sup>5</sup> M. Beck,<sup>6</sup> and D. A. Weitz<sup>1,†</sup>

<sup>1</sup>*Department of Physics and DEAS, Harvard University, Cambridge, Massachusetts 02138*

<sup>2</sup>*Unilever Research, Edgewater, New Jersey 07020*

<sup>3</sup>*Department of Physics and Astronomy, University of Pennsylvania, Philadelphia, Pennsylvania 19104*

<sup>4</sup>*Universität Konstanz, Fachbereich Physik, 78457 Konstanz, Germany*

<sup>5</sup>*Department of Chemical Engineering, Princeton University, Princeton, New Jersey 08544*

<sup>6</sup>*BASF AG, 67056 Ludwigshafen, Germany*

(Received 17 May 2001; revised manuscript received 7 September 2001; published 21 November 2001)

We develop a multiple particle tracking technique for making precise, localized measurements of the mechanical microenvironments of inhomogeneous materials. Using video microscopy, we simultaneously measure the Brownian dynamics of roughly one hundred fluorescent tracer particles embedded in a complex medium and interpret their motions in terms of local viscoelastic response. To help overcome the inherent statistical limitations due to the finite imaging volume and limited imaging times, we develop statistical techniques and analyze the distribution of particle displacements in order to make meaningful comparisons of individual particles and thus characterize the diversity and properties of the microenvironments. The ability to perform many local measurements simultaneously allows more precise measurements even in systems that evolve in time. We show several examples of inhomogeneous materials to demonstrate the flexibility of the technique and learn new details of the mechanics of the microenvironments that small particles explore. This technique extends other microrheological methods to allow simultaneous measurements of large numbers of probe particles, enabling heterogeneous samples to be studied more effectively.

DOI: 10.1103/PhysRevE.64.061506

PACS number(s): 83.85.Ei, 83.10.Pp, 82.35.Pq, 62.25.+g

### I. INTRODUCTION

Little is known of the mechanical microenvironments of complex materials such as polymer gels and the cytoplasm, yet understanding these local environments is critical for characterizing the microscopic processes that take place within them. Local measurements are necessary to explore the microscopic dynamics and mechanical properties that control many chemical and physical processes, such as the dynamics of colloidal particles in confined geometries, the diffusion of reactants for the chemical modification of gels, and the separation and transport of macromolecules and proteins in structured gels [1–4]. In biological materials, intercellular and intracellular transport, activities within cellular compartments, and the resistance encountered by molecular motors depend on local, not bulk, mechanical response to locally generated forces [5–8]. Often, the details of this microscopic response cannot be inferred from *in vitro* or bulk measurements. For example, intracellular biochemical reaction rates may differ significantly from those measured in dilute solution because macromolecular crowding and the physical constraints imposed by the cytoskeletal network dramatically alter the mobility of reactants [9–14]. In this paper, we present a technique to study local mechanical properties by simultaneously tracking many Brownian tracer

particles and using a combination of concepts of microrheology and precise statistical tools to describe the range of microenvironments encountered in a single system.

Macroscopically, rheological measurements completely describe the mechanical response of a material. Simple fluids are characterized by their viscosity and ideal elastic solids by their elastic modulus. Although more complex, viscoelastic materials that display properties of both solids and liquids can also be fully characterized by their frequency-dependent complex shear modulus. Microscopically, we can characterize the local mechanical response by a local viscosity and elasticity. However, we must also consider the ability of the large structures found in many complex materials to constrain small particles or macromolecules. At length scales where the constraining effects of these structures become important, the microscopic response is no longer connected to the bulk response by simple scaling laws, and direct local measurements are essential. In order to be interpreted in terms of mechanical microenvironments, these measurements should be local, should not depend on any assumptions about homogeneity, and should be sensitive to variations in local response and the presence of steric constraints.

A number of techniques have been employed to measure structure and dynamics in complex fluids. Static measurements, such as freeze fracture electron microscopy, x-ray diffraction, and fluorescence studies, give detailed structural information, but do not connect structure with dynamic mechanical response [2,15–17]. Fluorescence recovery after photobleaching (FRAP) experiments probe dynamics and measure the average long-time collective diffusion coefficient, but are insensitive to very local variations in response or constraining volumes [18–20]; thus, local measurements

\*Present address: Department of Chemical Engineering, University of Pennsylvania, Philadelphia, PA 19014.

†Author to whom correspondence should be addressed. FAX: 617-495-2875. Email address: weitz@deas.harvard.edu

are often preferable. For example, particle tracking experiments of individually fluorescently tagged lipids in the plasma cell membrane directly measure the diffusion of single lipids and reveal the localized interactions that give rise to the average trends measured with FRAP [21]. Recently, a similar technique has been used to measure the diffusion of proteins inside living cells [22].

Microrheology is another dynamic technique that can be used to probe very localized mechanical properties using tracer particles embedded in a complex fluid [23–25]. By using spherical tracer particles of a known size, particle motions can be interpreted quantitatively in terms of the local viscoelastic properties of the surrounding medium. While often interpreted in terms of the macroscopic bulk modulus, the real power of microrheology lies in the fact that individual tracer beads probe microenvironments and the motion of the individual tracer particles reflects the local mechanical response of the surrounding material. Typically in microrheology measurements, the tracer particles are much larger than the characteristic structures of the medium and particle motions are interpreted in terms of the linear frequency-dependent viscoelastic moduli. However, when the particle diameter is comparable to or smaller than the length scale of structures in the medium, the tracers can move within small cavities and their motions are not only a measure of the local viscoelastic response, but also of the effect of steric hindrances caused by the cavity walls. Thus, traditional microrheology techniques can be used to measure both local rheology and local constraining volumes in order to characterize fully the mechanical response of the microenvironments that small particles explore.

There are several different implementations of microrheology. One technique involves the active manipulation of embedded probe particles using optical or magnetic forces to move small probe particles and apply local stress to complex materials [26–31]. Although active measurements can be extremely useful, especially in stiff materials where large stresses are necessary to attain a measurable strain, applying a well-controlled force to the probe particle requires sophisticated instrumentation and calibration procedures. Additionally, large particles are often required to apply sufficiently well-controlled forces to the material, preventing the application of this technique to very small length scales.

Other microrheology techniques involve the passive observation of the thermal fluctuations of the probe particles. In this case, there are no limits on particle size, but the material must be sufficiently soft to allow detectable motion of particles moving with only  $k_B T$  of energy. In passive measurements, the key parameter is the mean-squared displacement of the tracer particles, and this can be measured by various methods. Dynamic light scattering techniques work well and report the mean-squared displacement averaged over an ensemble of tracer particles [24,32,33]. By contrast, single particle tracking microrheology uses a single probe particle to measure highly localized mechanical response [34–37] with high spatial and temporal sensitivity. Because this method uses a single probe instead of averaging over an ensemble, it is well suited to studying local microenvironments. However, in heterogeneous systems many repeated experiments with

different beads in different parts of the sample are required to completely characterize the material response. Another passive technique, two-particle microrheology, measures macroscopic properties in inhomogeneous samples by correlating the displacements of separated particles to measure the long wavelength thermal fluctuations of the material, but does not characterize different microenvironments directly [38]. None of the techniques allow for simultaneous local measurements in very heterogeneous samples, yet this is imperative for understanding microscopic processes in materials that evolve in time.

In this paper, we report an approach that uses video microscopy to simultaneously track roughly one hundred fluorescently labeled thermally activated particles in a single field of view. By analyzing the motions of the particles individually, we are able to perform many experiments in parallel. The strength of this technique lies in its experimental simplicity and our ability to collect large amounts of data in relatively short times. This allows us to directly probe and characterize heterogeneous microenvironments even in samples that are dynamically changing in time so that consecutive experiments are not possible.

There is, however, an intrinsic limitation in this technique: because of our finite imaging volume, the amount of data for any given particle is limited, reducing the statistical accuracy with which the mean-squared displacement can be determined. If we could collect sufficiently long trajectories, then the differences in the mean-squared displacements of different particles would be a direct measure of the variation in microenvironments found in the sample. However, our trajectories are not long enough to make precise individual measurements; thus, we are forced to use a more statistical approach. Rather than relying exclusively on the mean-squared displacement, we also develop statistical tools that allow us to use higher order statistics and compare distributions of displacements for individual particles. Using a formal statistical test to account for limited sampling, we determine which particles are measuring detectable differences in the local microenvironments. We group together indistinguishable particles and average over the mean-squared displacements of particles within the group to obtain more accurate measures of the local response for each grouping; we can thereby determine statistically meaningful variations throughout the sample. In samples where we detect spatial heterogeneity, we can measure the range of variation in local response and can physically map out the variations across the sample. We are thus able to identify and characterize different types of heterogeneity in samples with complex structures and dynamics.

To illustrate the flexibility and range of applicability of this technique, we examine three systems that display different types and ranges of heterogeneity. The first, a glycerol/water solution is purely viscous and homogeneous and is included as a benchmark to compare with more complex samples. The second sample is agarose, a fibrous polysaccharide gel that is characterized by many small pores that determine its utility as a common separation medium [16,17]. Agarose displays spatial heterogeneity and shows the importance of differentiating between length scales when measur-

ing mechanical response. Finally, a solution of the semiflexible biopolymer *F* actin, an important structural component of the cellular cytoplasm, is chosen as an example that illustrates the consequences of time-dependent fluctuations and their effect on small probe particles.

## II. EXPERIMENT

Fluorescent tracer particles were imaged with video microscopy epifluorescence (Leica DM-IRB/E) using a 100 $\times$ , oil-immersion objective with a numerical aperture of 1.4 at a magnification of 129 nm/CCD pixel. Video half frames were acquired to obtain tracer positions with 60 Hz temporal resolution. In each frame, the positions of the fluorescent particles were identified by finding the brightness averaged centroid position with a subpixel accuracy of approximately 10 nm [39]. The fluorescent beads appeared bright even as the particles moved slightly in and out of focus, allowing a more precise determination of the centroid position than is possible with nonfluorescently tagged particles. Samples were prepared with roughly one hundred particles visible in each field of view. Note that although better temporal and spatial resolution can be obtained with laser deflection particle tracking measurements of single particles [35], the resolution given by our simple video detection scheme is sufficient to study the dynamics of a wide range of soft materials. Furthermore, the ability to measure many particles simultaneously allows the determination of the dynamic correlations between neighboring particles and the local distribution of mechanical properties without numerous repeated experiments. This is particularly important for the study of samples that can evolve with time, where measurements must be done in a short period of time so that the aging has not modified the sample or its properties.

Ten minutes of video were recorded on S-VHS tape and digitized and analyzed offline, yielding a few million particle positions for each sample. We considered only particles that remain in focus for at least 5 s, to ensure minimal statistical accuracy for individual particles. This condition has the potential to bias our observed distributions by underweighting the fraction of fast-moving particles. However, for a typical solution with viscosity of 5 cp, the distance that a 0.5  $\mu\text{m}$  particle diffuses in 5 s is smaller than the depth of field, which is roughly 2  $\mu\text{m}$ ; thus we expect the effects of the biasing to be very small. In more viscous media, or in materials that constrain particles within local structures, the probability of a particle making a long excursion from the focal plane is even further reduced. Here, we consider only one-dimensional particle motion to maximize the accuracy of our tracking algorithms; since each video half frame consists of half as many rows as the full image, the accuracy is degraded in the direction perpendicular to the row direction [39]. Two-dimensional analysis of the particle tracks can also be done in cases when the anisotropy of the individual microenvironments is of importance.

Agarose (Seakem LE; FMC) was dissolved in 45 mM Tris buffer at pH=8 with 0.01% Triton X-100 surfactant at a concentration of 0.36% w/v and heated to boiling for approximately 1 min. The solution was cooled to 80  $^{\circ}\text{C}$ , above

the gelation temperature, and 500 nm diameter rhodamine-labeled carboxylate-modified latex polystyrene spheres (Molecular Probes) were added at a volume fraction of 0.2%. The solution was then injected into a heated chamber, consisting of a #1.5 coverslip and microscope slide. The chamber was hermetically sealed using UV-cured epoxy (Norland #81) and quench cooled to room temperature, triggering gelation of the agarose.

Actin prepared from rabbit muscle [40] and stored in *G* buffer [2 mM Tris-Cl, 0.2 mM ATP, 0.5 mM dithiothreitol (DTT), 0.2 mM  $\text{CaCl}_2$ ] was mixed with rhodamine-labeled 470 nm diameter tracers and polymerized in the sample chamber at a concentration of 1 mg/mL with the addition of KCl to 75 mM,  $\text{MgCl}_2$  to 2.5 mM, and *N*-2-hydroxyethylpiperazine-*N'*-2-ethane sulphonic acid (HEPES) to 10 mM. Phalloidin was added in a 1.2:1 molar ratio to *G* actin to stabilize the actin filaments.

## III. RESULTS AND DISCUSSION

Although we are ultimately interested in local microenvironments, the ensemble-averaged mechanical response gives valuable information about the dominant physics of the material. Using multiparticle tracking, millions of positions are assigned to thousands of particle trajectories, from which we calculate the ensemble-averaged mean-squared tracer displacement,  $\langle \Delta x^2 \rangle = \langle |x(t+\tau) - x(t)|^2 \rangle$ , as a function of lag time  $\tau$  where the angular brackets indicate an average over many starting times  $t$  as shown in Fig. 1. The beads in glycerol are purely diffusive, as expected for a simple fluid, and  $\langle \Delta x^2 \rangle$  is linear in  $\tau$ , as shown in Fig. 1(a). These data can be interpreted as a measure of viscosity  $\eta$  using  $\langle \Delta x^2(\tau) \rangle = 2D\tau$  in one dimension where  $D = k_B T / 6\pi\eta a$  and  $a$  is the tracer particle radius. The beads in agarose move significantly differently, as shown in Fig. 1(b). The particles show approximately diffusive behavior at short times; however, at the longest times, the mean-squared displacement appears to be approaching a plateau, indicating that the particles are becoming constrained. The *F* actin sample shows no true plateau, as shown in Fig. 1(c) and is subdiffusive for all accessible times, with power-law behavior having slopes well below one; this suggests that, while the beads are not permanently caged, their motions are affected by the surrounding network.

Although the ensemble response gives valuable insight into average mechanics, in order to characterize microenvironments, it is necessary to examine the individual particles directly. In Fig. 2 we show the time evolution of the mean-squared displacement of several individual particles for each system. There are very large variations from particle to particle. While it is tempting to explain different displacements by variations in the local microenvironments, it is not correct to do so. This is most clearly evidenced by the results for the glycerol solution; although the microenvironments are strictly homogeneous, the time-averaged mean-squared displacements show large deviations, as shown in Fig. 2(a). This reflects the fact that these data are not an appropriate measure of heterogeneity since individual particles are not sufficiently time averaged to determine a statistically accu-

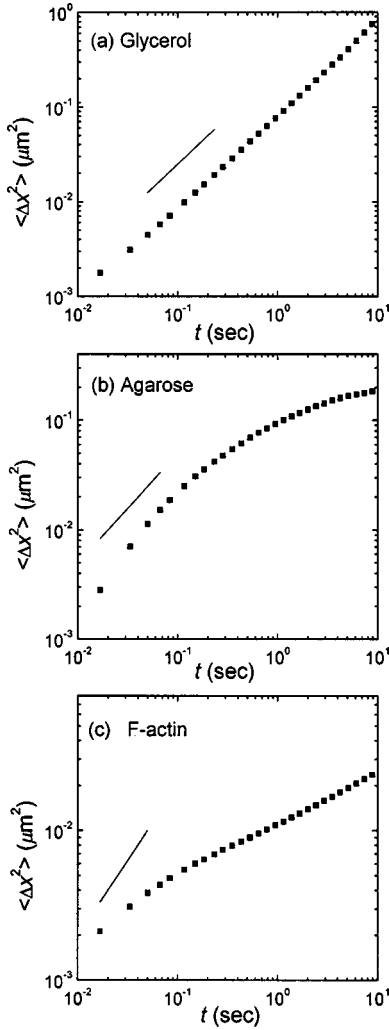


FIG. 1. Time- and ensemble-averaged mean-squared displacements as a function of time. The solid line in each figure indicates a slope of 1. (a) Glycerol:  $\langle \Delta x^2 \rangle$  is linear in time, as expected for a simple fluid. (b) Agarose: Tracer particles diffuse at short times and  $\langle \Delta x^2 \rangle$  is linear in time. At longer times, the particles are caged, and we observe the onset of a plateau:  $\langle \Delta x^2(\tau \rightarrow \infty) \rangle = 0.2 \mu\text{m}^2$  suggesting a plateau modulus of  $G = k_B T / \pi a \langle \Delta x^2(\tau \rightarrow \infty) \rangle \approx 0.1 \text{ Pa}$ . (c) *F* actin: The motion is subdiffusive at short times, and even further constrained at longer times.

rate mean-squared displacement; thus, at least part of the particle to particle variation is a result of poor statistics [41]. In the agarose sample, as shown in Fig. 2(b), the mean-squared displacements of the individual particles appear to vary much more than the particles in the glycerol sample, suggesting there may be a range of underlying microenvironments. The actin sample, as shown in Fig. 2(c), also displays variations in mean-squared displacements that are larger than those of the glycerol but not quite as large as those of the agarose. However, in order to make any quantitative comparisons, we must be careful to isolate the variations due to different local mechanical environments from the variations due to limited statistical sampling.

As evidenced most strikingly by the glycerol data, we do

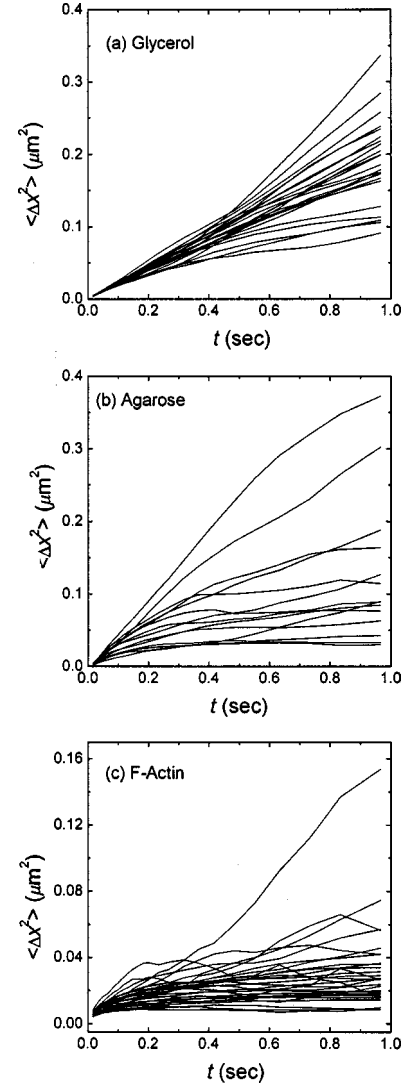


FIG. 2. Individual particle mean-squared displacements for several particles in (a) glycerol, (b) agarose, and (c) *F* actin. The spread of  $\langle \Delta x^2 \rangle$  reflects the uncertainties due to statistical fluctuations that result from short data collection times.

not have sufficient statistics to accurately determine the mean-squared displacements of the particles directly. Instead we use higher order statistics to better distinguish the effects of poor statistics from true variations in the sample. We examine the distribution of displacements at lag time  $\tau$ ,  $P(\Delta x, \tau)$ , known as the van Hove correlation function. The ensemble-averaged van Hove correlation function for the glycerol/water solution is shown for two different lag times, 0.033 s and 0.1 s, in Fig. 3(a). The lines are Gaussian fits to the data, and there is good agreement as expected for a purely diffusive system where the particle motion is described by a simple random walk, with  $P(\Delta x, \tau) = (4\pi D\tau)^{-1/2} \exp(-\langle \Delta x^2 \rangle / 4D\tau)$ . The variance of the distribution provides a measure of the diffusion coefficient, and hence, the viscosity. A sampling of van Hove correlation functions for individual particles at a lag time of 0.1 s is shown in Fig. 3(b). The solid lines indicate the Gaussian fit

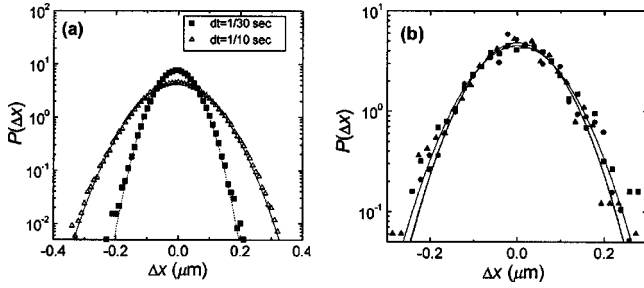


FIG. 3. van Hove correlation functions for particles moving in glycerol. (a) The ensemble-averaged data is fit by a Gaussian distribution over several orders of magnitude, as expected for a purely viscous fluid. (b) Individual particles, shown at a time lag of 0.1 s, also display Gaussian statistics, and measure the same diffusion coefficient, indicating the homogeneity of the solution. The small differences between the fits are due to limited statistics in the evaluation of  $P(\Delta x, t)$ .

to the distribution. The particles each follow Gaussian statistics and appear to be indistinguishable, indicating that each tracer bead experiences the same local diffusion coefficient; thus the solution is homogeneous. In fact, the Gaussian behavior of the ensemble-averaged van Hove correlation function is a strong indicator of the homogeneity of the solution, since the sum of the individual particle data will be Gaussian only if each particle displays Gaussian statistics, and each has the same diffusion coefficient.

Although qualitative comparisons are possible by observing the shapes of the van Hove correlation functions, for statistically accurate comparisons of the individual particle data, we use a more formal test. One useful parameter is the  $F$  statistic,  $f = (\sigma_k^2/n_k)/(\sigma_l^2/n_l)$ , which compares the variances of any two independent, random, normally distributed quantities, distinguished by labels  $k$  and  $l$ , with variance  $\sigma^2$  and  $n$  degrees of freedom [42,43]. For particle trajectories,  $n$  is the number of statistically independent time steps that build up the van Hove correlation function. For time series  $x(t)$  of duration  $T = m\delta$ , sampled to  $x(t_i)$ ,  $t_i = i\delta$ , assembling  $P(\Delta x^2, \tau = j\delta)$  from  $m/j$  nonoverlapping segments will give  $n = m/j$  degrees of freedom. However, this sampling procedure discards a large fraction of our data. Alternatively, we can assemble  $P(\Delta x, \tau = j\delta)$  from every pair  $[x(t_i), x(t_{i+j})]$  to produce better statistics but such sampling does not produce  $n = m - j$  degrees of freedom because sequential pairs are not statistically independent. In order to determine the number of independent degrees of freedom in such oversampled data, we perform Monte Carlo simulations of an ensemble of particles, where each experiences the same local diffusion coefficient. We calculate the van Hove correlation functions for each particle, and calculate the  $F$  statistic for each pair. Empirically, we find that the  $F$  statistic derived from oversampled data is very nearly  $F$  distributed with  $n = 1.5m/j$ , and we use this relationship to determine the number of independent degrees of freedom in our data.

To make statistically accurate comparisons of individual particles, we use the  $F$  test, which compares the variances of two distributions using the  $F$  statistic and returns the confi-

dence level with which we can determine the two distributions to be statistically different. In some soft materials, neighboring particles show correlated motion due to long-range hydrodynamic or viscoelastic effects [38]; however, because every particle is influenced by many neighboring particles, we expect any correlations to cancel out in the distribution of displacements for a single particle. Thus we expect the individual van Hove correlation functions to be statistically independent, and the variances of these distributions to be  $F$  distributed. Our ability to make meaningful distinctions using the  $F$  test depends upon the number of independent events that build up the individual distributions. For the materials studied here, we found that a particle volume fraction of roughly 0.001 and observation times of 5–20 min were sufficient to gather enough data to make meaningful comparisons. At these volume fractions we do not expect the presence of the particles to alter network formation; consistent with this, our results do not depend on particle volume fraction. For softer or less viscous materials, we expect increased particle motion and require a lower volume fraction of particles in order to ensure that the interparticle spacing is greater than the distance a particle moves between subsequent frames, thus allowing a unique identification of each particle at each time step. Lower magnification optics will capture a larger field of view, and may be useful for measurements in such materials; however, the apparent size of individual particles must be at least five pixels to ensure accurate tracking of the center of brightness. Additionally, longer observation times may be required to gather sufficient statistics since particles in softer materials are more likely to move out of the field of view.

Using a 95% certainty of difference, we compare particles pairwise to identify those particles that are statistically distinguishable. Unlike other methods, which present only distributions of statistical behaviors, using the  $F$  test we are able to make actual comparisons of individual particle tracks. We then group the particles into “clusters” where all the particles in a given cluster are statistically indistinguishable. The beads in the glycerol/water solution group into only one cluster, as expected for a homogeneous solution where all particles measure the same local viscosity. Thus, despite the large apparent variation in the mean-squared displacements, the statistics are nevertheless sufficiently good to show that there is in fact only a single microenvironment; however, we must perform this more careful statistical analysis to determine this.

By contrast, in agarose, the beads display markedly different behavior, reflecting the complex nature of the medium. Agarose is known to be structurally heterogeneous, consisting of a complex network of fibrous molecules [16]. We measure the macroscopic elastic plateau modulus to be roughly 2700 Pa, using a strain-controlled rheometer (Ares; Rheometrics) for frequencies from 0.01–100 rad/s. In a homogeneous material, this shear modulus would be too large to produce a detectable amount of motion with thermally activated tracer particles. The calculated mean-squared displacements for a 1- $\mu\text{m}$ -diameter particle in the agarose would be 1 nm<sup>2</sup>, which we cannot resolve with our particle tracking method; consistent with this, we observe that beads

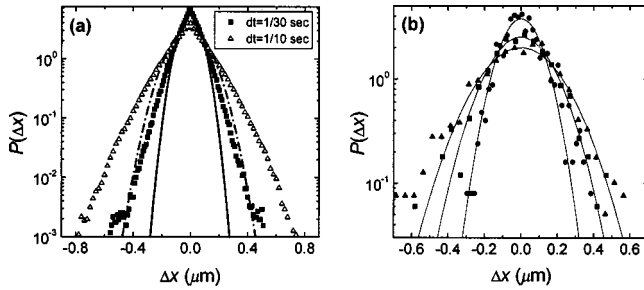


FIG. 4. van Hove correlation functions for particles moving in agarose. (a) The ensemble-averaged distribution is non-Gaussian for even small displacements at all time lags, and is approximately described by an exponential distribution. (b) Individual particle distributions, shown at a time lag of 0.1 s, are each fit by a Gaussian of a different width, indicating a different local diffusion coefficient.

that are 1  $\mu\text{m}$  in diameter do not move detectably, indicating that the particles are larger than the characteristic elastic structures and probe the bulk elastic response. However, while agarose does contain large elastic structures that span the sample and bear stress macroscopically, at short length scales, these structures do not form a homogeneous elastic continuum; instead, agarose is characterized by many smaller voids, or pores, through which smaller particles may move [17]. By observing the dynamics of the smaller particles, we can characterize the mechanical microenvironments of the pores themselves.

Although constrained, the smaller particles move within the irregularly shaped pores, and do move in and out of focus, limiting our ability to track an individual particle for long times. Because we are limited by trajectories of finite length, we again use higher order statistics to make quantitative comparisons. The ensemble-averaged van Hove correlation function is shown in Fig. 4(a) at a time lag of 0.033 s and 0.1 s. The lines indicate the Gaussian fit to each distribution; however, unlike the homogeneous glycerol solution, the agarose data deviates from the Gaussian fit at all displacements at both time lags. These deviations from Gaussian behavior indicate a detectable heterogeneity in mechanical response. A sampling of the individual van Hove correlation functions at a lag time of 0.1 s is shown in Fig. 4(b), and the Gaussian fit for each distribution is indicated by a solid line. Within our limited statistical accuracy, the distribution of particle displacements for each bead appears to be Gaussian; however, the widths of the distributions are different, reflecting different local diffusion coefficients.

At short lag times, where the statistical accuracy is best, the  $F$  test identifies several statistically different groups of particles, indicating microscopic differences in the local properties. However, at longer lag times, where the particles are more constrained, we are unable to distinguish any differences in the distributions with the  $F$  test. In this long time limit, the number of independent time steps is considerably lower, decreasing the statistical accuracy of the comparison. However, there are still wide variations in the mean-squared displacements; thus, in order to better characterize the long-time behavior, we average the data in a statistically meaning-

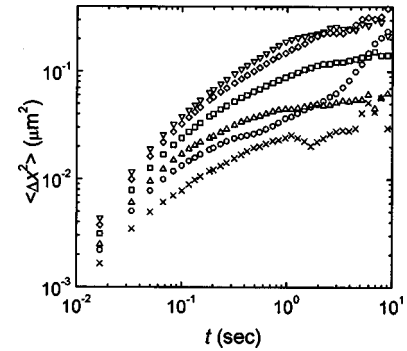


FIG. 5. Cluster-averaged mean-squared displacement for 500 nm particles in agarose. The local viscosity ranges from 2.3–8.6 cp and the pore sizes from 700–1200 nm. There is a correlation between short-time viscosity and the long-time plateau in the mean-squared displacement due to increased hydrodynamic resistance in the smallest pores.

ful way. We use the  $F$  test results to group the particles into clusters according to their local viscosity based on the distributions at short times and average the mean-squared displacements over the particles in each cluster. Because all particles in a given cluster are statistically indistinguishable and measure the same microscopic response, they form a meaningful ensemble and it is appropriate to consider the behavior averaged over particles in the cluster. The cluster-averaged mean-squared displacements for the six most populated clusters are shown in Fig. 5. At short times, the motion is very nearly diffusive and we measure a range of local viscosities from 2.3–8.6 cp. At long times the cluster-averaged mean-squared displacements do not converge, suggesting that particles in different clusters do experience different microenvironments.

The plateau in the mean-squared displacement at long times indicates that the particles are constrained by the material but we require further tests to reveal the nature of this constraint. In a homogeneous medium, the plateau is interpreted in terms of the elastic modulus of the material; however, in a heterogeneous microenvironment, the plateau may be a measure of local elasticity, or a measure of the size of the local constraining volume, or pore. To differentiate between these two possibilities, we use probe particles of different sizes and determine how  $\langle \Delta x^2(\infty) \rangle$  scales with particle radius  $a$ . If the plateau is a measure of local elasticity  $G$  then  $\langle \Delta x^2(\infty) \rangle = kT/\pi Ga$ , so  $\langle \Delta x^2(\infty) \rangle$  scales with  $1/a$ . If, however, the plateau is a measure of pore size  $d$  then  $d = a + h$ , where  $h$  is the size of the fluid filled gap between the particle surface and the pore wall and is approximated by  $h = [\langle \Delta x^2(\infty) \rangle]^{1/2}$ . We have repeated our measurements with 200 nm particles, and compared the results with those obtained with 500 nm particles. We find that  $\langle \Delta x^2(\infty) \rangle$  does not scale with particle size; instead  $a + [\langle \Delta x^2(\infty) \rangle]^{1/2}$  remains roughly constant. This implies that in agarose the plateau in the mean-squared displacement does not provide a measurement of local elasticity, instead it probes the average pore size, which is found to be approximately 1  $\mu\text{m}$ .

Once we have determined the nature of the constraint that

gives rise to the long time plateau, we can begin to characterize and compare the microenvironments in agarose. The cluster-averaged mean-squared displacements suggest that the particles that are the most tightly constrained at longer times experience the highest local viscosity at earlier times. The plateau in mean-squared displacement is a measure of an effective pore size, and our data suggest that particles in smaller pores are diffusing more slowly; this may be due to hydrodynamic effects. Particles moving in fluid-filled pores will experience an apparent increase in viscosity since in order to move, the particle must squeeze fluid out of a thin gap between the particle surface and the pore wall. A particle of size  $a$  moving in a fluid-filled pore of size  $a+h$ , where  $h \ll a$ , will experience a drag force  $F = 3\pi\eta a^4/2h^3$  and an effective diffusion coefficient of  $D = 2k_BTh^3/3\pi\eta a^4$  [44]. If we assume spherical, impermeable pores and again estimate the pore size by assuming  $h \approx (\langle \Delta x^2(\infty) \rangle)^{1/2}$ , we find that for the smallest pores, where the approximation  $h \ll a$  is most valid, the measured increase in viscosity is consistent with increased hydrodynamic resistance. In reality, the pore walls are likely irregular, fibrous and semipermeable, giving rise to complex flow fields and long-range hydrodynamic effects. Nonetheless, our data suggest that the walls do decrease the mobility of the particles they constrain and further this simple scaling relation describes the general trend we observe.

To verify the effects of pore size on the diffusivity of small particles, we examine the behavior of the 200 nm particles, which should be less sensitive to hydrodynamic effects. In this case, we again distinguish several clusters of particles that experience different microenvironments; however, we measure a smaller range of local viscosities, from 2.4–3.7 cP, in agreement with the viscosities measured by the least constrained 500 nm particles. This suggests that the pores are filled with a soft polymer that raises the viscosity to 2–3 times that of water; however, hydrodynamics do play a role in further decreasing the diffusivity of the 500 nm particles in the smallest pores.

To better characterize the range of microenvironments present in the sample, we do Monte Carlo simulations of an ensemble of beads performing random walks with a known distribution of local diffusion coefficients. We use the same particle trajectory lengths that we measure experimentally to ensure the same statistical limitations and vary the width of the distribution of local diffusion coefficients until we recover the same clustering behavior found experimentally. Our data is consistent with a distribution of diffusion coefficients that varies by  $20 \pm 5\%$ . Both the cluster analysis and the Monte Carlo simulations show that despite the large contrast between macroscopic and microscopic environments, the range of mechanical microenvironments within the pore structure is quite small. This result could not have been predicted from bulk measurements alone and emphasizes the importance of direct local measurements.

We can further investigate the nature of the microenvironments by plotting the trajectories of all particles and color coding the individual tracks according to cluster membership as shown in Fig. 6. This allows us to physically map the variation in local mechanical response across the sample and

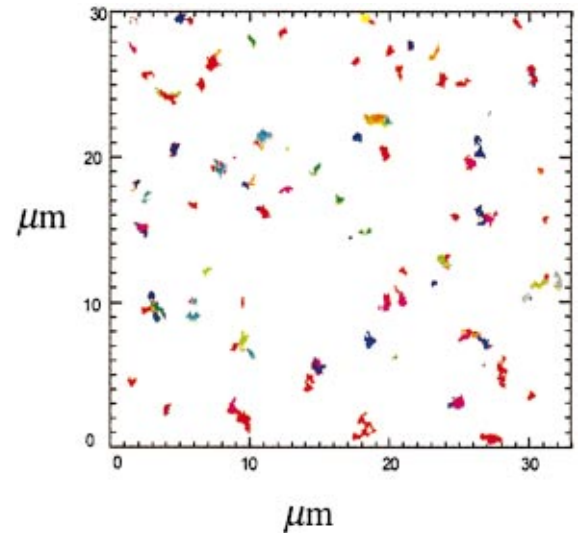


FIG. 6. (Color) The particle trajectories for the agarose gel give a spatial map of mechanical microenvironments. The trajectories are color coded according to cluster analysis; beads of the same color experience the same local viscosity. There is no long-range spatial correlation, suggesting that the length scale of heterogeneity is small—of the order of a particle diameter.

to look for spatial correlations of similar microenvironments. We observe no long-range spatial correlations indicating that, in agarose, the length scale of heterogeneity is small, and nearby pores have different sizes and are characterized by different local viscosities.

To further test the flexibility of this technique, and to explore the effect of time-dependent fluctuations on small probe particles, we measure individual particles moving in a solution of  $F$  actin. The embedded tracer particles are 470 nm in diameter, slightly larger than the average mesh size of approximately 300 nm expected for a 1 mg/mL solution of  $F$  actin [45]. Unlike the beads in agarose, however, the tracer particles in actin are constrained by the semiflexible polymer network but are not permanently caged or confined in pores. The ensemble-averaged van Hove correlation function shows roughly Gaussian behavior at shortest lag time of 0.033 s, but deviates at slightly longer time lags, above 0.1 s, to give a broader tail as shown in Fig. 7(a). Such non-Gaussian behavior indicates that the system is not a simple homogeneous solution at the length scale of the probe particles. The van Hove correlation functions of individual particles at a time lag of 0.1 s are shown in Fig. 7(b). The distributions look similar for small displacements, although there is deviation at larger displacements and some indication of non-Gaussian behavior; however, this must be viewed with caution given the poor statistics.

Our attempts to use the  $F$  test to classify particles by statistically different diffusivities failed to identify any distinguishable clusters. Our inability to distinguish between individual particles despite the non-Gaussian behavior of the ensemble-averaged distribution suggests the possibility of a temporal heterogeneity. In this case, the time-averaged response of even an individual particle may be a superposition

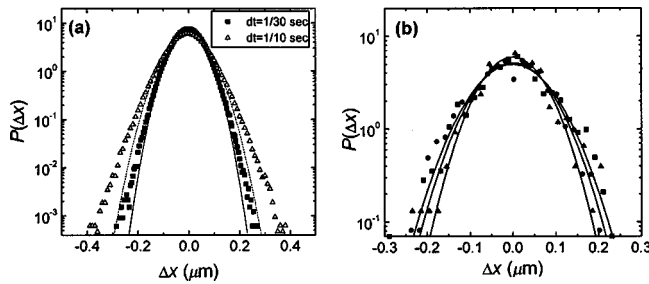


FIG. 7. van Hove correlation functions for particles moving in actin. (a) The ensemble-averaged distributions do not compare well to a Gaussian fit. There are far too many large displacement events for a Gaussian displacement model, a deviation that grows with time. (b) Individual particle distributions, shown at a time lag of 0.1 s are similar, although there are differences for larger displacements.

of data from several microenvironments. Such a superposition would result in a more complicated form for the van Hove correlation function of an individual particle; however, our limited statistical accuracy does not allow us to distinguish any difference. Preliminary work in our laboratory suggests that a single particle that is roughly equal in size to the average mesh size can in fact sample several different cages formed by the *F* actin network, and can even “jump” repeatedly between two neighboring cages [46]. This suggests that the temporal heterogeneity may be due to the actin network rearranging in time, or the beads exploring different static microenvironments over the course of the measurement, or both, resulting in a time-averaged response that is not necessarily a simple representation of any of the instantaneous microenvironments. The characteristic crossover frequency from viscous to elastic behavior for similar *F* actin solutions has been reported in the range of 0.1–1 Hz [47], corresponding to approximately the same time lags we are investigating and indicating the ability of the network to rearrange on this time scale.

The ability of probe particles to move between different microenvironments in a fluctuating network is consistent with previous measurements in actin, where small particles have reportedly failed to measure bulk mechanical response [38,47–49]. One explanation for this failure is that probe particles that are much smaller than the persistence length of the actin filaments, typically 10–20  $\mu\text{m}$ , introduce nonaffine deformations of the network as filaments are bent around the probes with a characteristic radius comparable to the bead diameter [47,48]. This nonaffine excitation results in a different elastic response than is measured in macroscopic rheology. This effect is very sensitive to filament length, and the wide distribution of filament lengths that our samples likely possess could cause mechanical heterogeneity if the small particles are able to move through different microenvironments characterized by different average filament lengths during the measurement. Furthermore, although reptation of filaments typically occurs on time scales of 1000 s, much longer than the time scales of our measurements, the relaxation time might be considerably shorter if short filaments dominate the local response. The resultant distribution of re-

laxation times could also give rise to temporal heterogeneity.

A recent comparison of one- and two-particle microrheology in actin samples also showed that the mean-squared displacement calculated from the “self-diffusion” of a single probe particle is probably not solely a measure of the fluctuation spectrum of the actin network [38]. Rather, the mean-squared displacement likely reflects a superposition of the long wavelength thermal undulations of the polymer network and the local motion of the particle inside a transient “cage” formed by the surrounding actin filaments. This local motion could give rise to temporal heterogeneity if the average spacing between filaments fluctuates in time, or if a particle samples several different cages during the course of the measurement. These results may be important to help rationalize previous measurements in actin where particles had been assumed to measure a homogeneous network response.

#### IV. SUMMARY

In this paper, we have described a multiparticle tracking technique that investigates mechanical microenvironments of complex systems at the micron scale. Such local measurements are essential to fully characterizing inhomogeneous systems, and are imperative to understanding the microscopic processes that occur in structured materials. By simultaneously tracking multiple particles moving in complex solutions, we can perform measurements even in time-evolving samples, such as gels undergoing polymerization and the cytoplasm of living cells. Although the finite imaging volume limits the statistical accuracy with which we can calculate the mean-squared displacement of individual particles, by adopting a more statistical approach, we can compare distributions of particle displacements to identify quantitative differences in local microenvironments.

In agarose, large fibrous polymers form heterogeneous elastic structures that bear macroscopic stress but allow the motion of particles in confined pores. By examining statistics of individual particles and clustering those particles that are statistically indistinguishable, we measure variations in the properties of the pores and physically map those variations across the sample. Despite the significant differences between macroscopic rheological properties and the microscopic environment explored by small particles, the variation within local microenvironments is quite small, of order 20%. We do not observe spatial correlation of similar microenvironments, indicating that neighboring pores have different sizes and local viscosities. Furthermore, we detect a decrease in the mobility of particles in the smallest pores due to increased hydrodynamic drag. These results highlight the importance of measuring mechanical response at different length scales in highly structured heterogeneous materials. For instance, small macromolecules can easily move through the pores of the gel but large complexes of several macromolecules may be dramatically slowed or even trapped.

In actin, we find signatures of heterogeneity in the ensemble-averaged distributions of particle displacements, but are unable to statistically distinguish any individual particles. We interpret this result as evidence of temporal hetero-

geneity, and suggest that individual particles may explore several different microenvironments during the course of the measurement. The ability of particles to move through different mechanical environments over short times may impact the previous interpretation of actin microrheology experiments that have been interpreted in terms of bulk rheological response. Furthermore, the ability of the multiparticle tracking technique to identify temporal heterogeneity may allow

the measurement of characteristic time scales in structurally complex systems that dynamically change in time.

#### ACKNOWLEDGMENTS

The authors gratefully acknowledge support from Unilever, and from the NSF (DMR-9971432), the Materials Research Science and Engineering Center through the auspices of the NSF (DMR-9809363), and NASA (NAG3-2284).

- 
- [1] N. Tamai, M. Ishikawa, N. Kitamura, and H. Masuhara, *Chem. Phys. Lett.* **184**, 398 (1991).
- [2] G. Greiss, K. B. Guiseley, and P. Serwer, *Biophys. J.* **65**, 138 (1993).
- [3] D. F. Evans and H. Wennerström, *The Colloidal Domain: Where Physics, Chemistry, Biology, and Technology Meet* (VCH, New York, 1994).
- [4] M. Ciszowska and M. D. Guillaume, *J. Phys. Chem. A* **103**, 607 (1999).
- [5] K. Luby-Phelps, F. Lanni, and D. L. Taylor, *Annu. Rev. Biophys. Chem.* **17**, 369 (1988).
- [6] K. Luby-Phelps and D. L. Taylor, *Cell Motil. Cytoskeleton* **10**, 28 (1988).
- [7] D. W. Provan, A. McDowall, M. Marko, and K. Luby-Phelps, *J. Cell. Sci.* **106**, 565 (1993).
- [8] L. W. Janson, K. Ragsdale, and K. Luby-Phelps, *Biophys. J.* **71**, 1228 (1996).
- [9] H. A. Kramers, *Physica (Utrecht)* **7**, 284 (1940).
- [10] S. B. Zimmerman and A. P. Minton, *Annu. Rev. Biophys. Biomol. Struct.* **22**, 27 (1993).
- [11] M. Arrio-Dupont, S. Cribier, G. Foucault, P. F. Devaux, and A. d'Albis, *Biophys. J.* **70**, 2327 (1996).
- [12] M. Arrio-Dupont, G. Foucault, M. Vacher, P. F. Devaux, and S. Cribier, *Biophys. J.* **78**, 901 (2000).
- [13] D. J. Odde, *Biophys. J.* **73**, 88 (1997).
- [14] A. Srivastava and G. Krishnamoorthy, *Arch. Biochem. Biophys.* **340**, 159 (1997).
- [15] T. K. Attwood and D. B. Sellen, *Biopolymers* **29**, 1325 (1990).
- [16] T. K. Attwood, B. J. Nemes, and D. B. Sellen, *Biopolymers* **27**, 201 (1988).
- [17] N. Pernodet, M. Maaloum, and B. Tinland, *Electrophoresis* **18**, 55 (1997).
- [18] L. Hou, F. Lanni, and K. Luby-Phelps, *Biophys. J.* **58**, 31 (1990).
- [19] J. D. Jones and K. Luby-Phelps, *Biophys. J.* **71**, 2742 (1996).
- [20] E. M. Johnson, D. A. Berk, R. K. Jain, and W. M. Deen, *Biophys. J.* **70**, 1017 (1996).
- [21] M. J. Saxton and K. Jacobson, *Annu. Rev. Biophys. Biomol. Struct.* **26**, 373 (1997).
- [22] M. Goulian and S. M. Simon, *Biophys. J.* **79**, 2188 (2000).
- [23] F. C. MacKintosh and C. F. Schmidt, *Curr. Opin. Colloid Interface Sci.* **4**, 300 (1999).
- [24] T. G. Mason and D. A. Weitz, *Phys. Rev. Lett.* **74**, 1250 (1995).
- [25] A. J. Levine and T. C. Lubensky, *Phys. Rev. Lett.* **85**, 1774 (2000).
- [26] F. Ziemann, J. Rädler, and E. Sackmann, *Biophys. J.* **1994**, 2210 (1994).
- [27] F. Amblard, A. C. Maggs, B. Yurke, A. N. Pargellis, and S. Leibler, *Phys. Rev. Lett.* **77**, 4470 (1996).
- [28] F. G. Schmidt, F. Ziemann, and E. Sackmann, *Eur. Biophys. J.* **24**, 348 (1996).
- [29] M. T. Valentine, L. E. Dewalt, and H. D. Ou-Yang, *J. Phys.: Condens. Matter* **8**, 9477 (1996).
- [30] L. A. Hough and H. D. Ou-Yang, *J. Nanoparticle Research* **1**, 494 (1999).
- [31] A. R. Bausch, W. Möller, and E. Sackmann, *Biophys. J.* **76**, 573 (1999).
- [32] T. Gisler and D. A. Weitz, *Phys. Rev. Lett.* **82**, 1606 (1999).
- [33] A. Palmer, T. G. Mason, J. Xu, S. C. Kuo, and D. Wirtz, *Biophys. J.* **76**, 1063 (1999).
- [34] F. Gittes, B. Schnurr, P. D. Olmsted, F. C. MacKintosh, and C. F. Schmidt, *Phys. Rev. Lett.* **79**, 3286 (1997).
- [35] T. G. Mason, K. Ganesan, J. H. vanZanten, D. Wirtz, and S. C. Kuo, *Phys. Rev. Lett.* **79**, 3282 (1997).
- [36] B. Schnurr, F. Gittes, F. C. MacKintosh, and C. F. Schmidt, *Macromolecules* **30**, 7781 (1997).
- [37] S. Yamada, D. Wirtz, and S. C. Kuo, *Biophys. J.* **78**, 1736 (2000).
- [38] J. C. Crocker, M. T. Valentine, E. R. Weeks, T. Gisler, P. D. Kaplan, A. G. Yodh, and D. A. Weitz, *Phys. Rev. Lett.* **85**, 888 (2000).
- [39] J. C. Crocker and D. G. Grier, *J. Colloid Interface Sci.* **179**, 298 (1996).
- [40] J. D. Pardee and J. A. Spudich, *Methods Enzymol.* **85**, 164 (1982).
- [41] H. Qian, M. P. Sheetz, and E. L. Elson, *Biophys. J.* **60**, 910 (1991).
- [42] B. R. Martin, *Statistics for Physicists* (Academic, London, 1971).
- [43] B. P. Roe, *Probability and Statistics in Experimental Physics* (Springer-Verlag, New York, 1992).
- [44] D. J. Acheson, *Elementary Fluid Dynamics* (Oxford University Press, Oxford, 1990).
- [45] C. F. Schmidt, M. Bärmann, G. Isenberg, and E. Sackmann, *Macromolecules* **22**, 3638 (1989).
- [46] M. Gardel, I. Wong, A. Bausch, and D. A. Weitz (unpublished).
- [47] F. G. Schmidt, B. Hinner, and E. Sackmann, *Phys. Rev. E* **61**, 5646 (2000).
- [48] A. C. Maggs, *Phys. Rev. E* **57**, 2091 (1998).
- [49] D. C. Morse, *Macromolecules* **31**, 7044 (1998).